Understanding Trade-offs of Phase Change Materials for Transient Thermal Mitigation

Lauren Boteler, Michael Fish, Morris Berman, and Justin Wang
U.S. Army Research Laboratory
Adelphi, MD, USA, 20783
Email: lauren.m.boteler.civ@mail.mil

ABSTRACT

There are many applications throughout the military and commercial industries whose thermal profiles are dominated by intermittent and/or periodic pulsed thermal loads. Typical thermal solutions are steady state heat sinks that provide enough continuous cooling capacity to address the peak thermal load as if it were a steady-state condition. Such a conservative approach guarantees satisfying the thermal challenge, but it can result in significant cooling overdesign. This work investigates improving system size and weight without sacrificing platform performance by developing a package focused on transient thermal mitigation using time-scale matched (TSM) phase change materials (PCMs). The TSM PCMs comprise both metallic and organic PCMs that enable each other. This work demonstrates that for short pulses, metallic PCMs have a fast thermal response due to their high thermal conductivity (high-k) but their weight, cost, and integration complexity limits their viability in applications. Alternatively, organic PCMs are inexpensive, lightweight, and can have very high latent heat of fusion but have very low thermal conductivity (low-k) compared to metals and thus cannot absorb heat quickly. The concept of time-scale matching will be presented as well as a numerical study outlining design trade-offs, packaging considerations, and the five time scale matching regimes. The paper will conclude with a Monto Carlo analysis showing a Pareto front of the optimal solutions when integrating copper, a metallic PCM and an organic PCM simultaneously and the solution families that are created.

KEY WORDS: time scale matching, transient thermal, metallic phase change materials, gallium, latent heat, PCMs, pulsed power applications, low melting temperature alloy, thermal management, thermal buffering

NOMENCLATURE

E	energy, J
V	volume, cm^3
c_p	specific heat (J/kgK)
T	temperature, °C
L	latent heat (J/cm^3)
S	solid
L	liquid

Greek symbols

ρ	mass density (kg/m^3)
Δ	delta, change in

INTRODUCTION

There are many applications whose thermal profiles are dominated by intermittent and/or periodic pulsed thermal loads including vehicles, RF systems, computational sprinting, laser weapons, etc. In many of these applications, it is the electronics packaging and thermal management which limits device performance. In power electronics for example, in most cases the power devices must be derated and they cannot achieve their full rating due to the thermal/packaging challenges [1]. Additionally, current thermal management typically designs for the worst-case peak load conditions resulting in a conservative solution with significant cooling overdesign. This research focuses on developing a thermal solution which designs for the average thermal load instead of the peak. By implementing a system capable of providing sufficient cooling capacity during the pulsed load and dissipating that heat prior to onset of another thermal event, the system can be designed for a capacity closer to the average thermal power level rather than the peak. This enables significant system size and weight reductions without sacrificing platform performance through the use of phase change materials (PCMs). The amount of energy (E_{total}) that any volume of material (V) can absorb over a given change in temperature (ΔT) is given by Equation 1 given the materials properties of density (ρ), specific heat (c_p) and latent heat (L).

$$E_{total} = \underbrace{V\rho c_p \Delta T}_{\text{Specific Heat}} + \underbrace{VL}_{\text{Latent Heat}} \quad (1)$$

Typical steady state thermal solutions focus on better heat sinks and high thermal conductivity materials (ex. copper). However, for transient applications, there needs to be a fundamental shift in thermal/packaging technology which specifically addresses the pulsed nature of the application. Fig. 1 compares the energy absorption in Joules (J) of copper, gallium (low melting temperature metal), and a commercially available paraffin (PT29) using Equation 1.

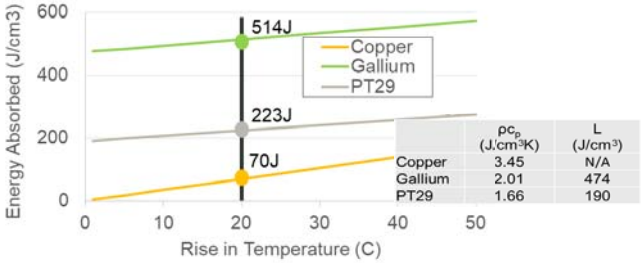

Fig. 1. Comparison of energy absorption between copper, gallium, and paraffin (PT29).

For a ΔT of 20°C, there is 3X and 7X more energy that can be absorbed by paraffin (PT29) and gallium, respectively, than by copper. This calculation is based on the criteria that the PT29 and gallium completely change phase (solid to liquid melt at 29°C) during which time, a significant amount of heat is absorbed.

This analysis in Fig. 1 is simplified in that it doesn't take into account the thermal conductivity, weight, cost, and integration complexity of each of these materials. Nor does it account for where and how these materials will be placed into the electronics assembly or the magnitude and duration of the thermal pulse. All of these factors play a role in the effectiveness of these materials and this paper will start to answer some of these design questions.

Most current PCM research focuses on organic (o-) PCMs (paraffin, sugar alcohols, etc.) for thermal buffering due to their low cost and ease of implementation. But due to their inherent low thermal conductivity, a significant amount of research has focused on improving the thermal conductivity of the organics through thermal enhancements such as metal mesh [2, 3], metal foams [4], heat sinks [5], carbon nanotubes [6] and metal honeycombs [7] high thermal conductivity foams, fins, porous media, etc. Several recent material reviews have highlighted metallic PCMs as likely candidates for phase change applications where system weight is less of a concern than high heat transfer rates [8, 9]. In addition, recent PCM selection and figure of merit analyses have highlighted low melting temperature metals as promising PCM candidates [10, 11, 12] A few research groups, including the authors of this paper, have been investigating metallic (m-) PCMs due to their high thermal conductivities and increased thermal responsiveness [13, 14, 15, 16]. However there has not been work addressing how the metallic PCMs and organic PCMs can work together.

This work focuses on time-scale matched PCMs which incorporate metallic PCMs in conjunction with organic PCMs to leverage the benefits of each material. Time-scale matching allows the high-k metallic PCMs to quickly absorb the initial portion of the pulse (primary melt) while accommodating the slower heating of the low-k organic PCMs until they also melt (secondary melt). The heat transfer process is broken down into 5 distinct regimes after the thermal pulse is initiated: (1) sensible heating of both the m-PCM and o-PCM (2) melting of the m-PCM, sensible heating of the o-PCM (3) melting of the m-PCM and o-PCM (4) sensible heating of the liquid m-PCM and melting of the o-PCM and (5) sensible heating of the liquid m-PCM and o-PCM.

MODELING TOOL

The effort will focus on methodologies for leveraging the advantages of o-PCMs and m-PCMs against the deficits of both. The ARL ParaPower tool is used for this analysis which has been validated and used previously to develop an understanding of single material PCM systems. ARL ParaPower is a parametric modeling tool which was co-developed by the U.S. Army Research Laboratory and the U.S. Naval Academy to enable co-design of electrical packages and an understanding of the tradeoffs across the electrical, thermal and mechanical domains. The model uses a 3D thermal resistance network to quickly calculate the temperatures and stresses in any rectilinear geometry [17, 18]. Previous work by the authors compared the ARL ParaPower tool to standard finite element analysis (FEA) showing <2 °C temperature difference and <30% error in stress while allowing >100X faster solution times [17].

The model allows input of 3D features through the use of (x, y, z) coordinates and each can be defined as either a solid, phase change material or internal boundary cavity (IBC). In Fig. 2, the yellow and blue portions each represent a feature which is subdivided into three elements. Heat fluxes and heat transfer coefficients are applied as boundary conditions.

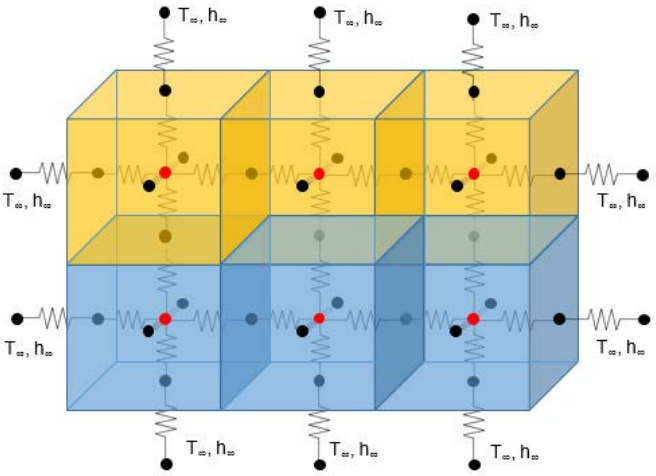

Fig. 2. Depiction of the 3D thermal resistance network used in the ARL ParaPower tool

A 3D network of thermal resistors is generated based on this geometry as shown in Fig. 2. A nodal summation is performed around each node, based on Equation 2. Every element has an equation which is compiled into a coefficient matrix. The power vector [Q] is also generated and a [T] vector is solved which equates to the temperatures in each element.

$$\sum_{i=1}^{6}\left(\frac{1}{R_i}\left(T_i^{p+1}-T_0^{p+1}\right)\right)-CT_0^{p+1}=-Q_0-CT_0^{p}$$

$$\text{where}\qquad C=\frac{\rho_0^p c_0^p V_0}{\Delta t} \qquad (2)$$

PCM melting has been incorporated into the tool in collaboration with Texas A&M University by defining a melt fraction (Φ) to each element. An energy balance equation is performed on each node and its melt fraction is updated at each time step. A full validation of the PCM portion of the tool can be found in [19]. All analyses in this paper will be performed using the ARL ParaPower tool.

MODELING DESCRIPTION

Understanding and exploiting the interdependencies between a pulsed heat source and multiple PCMs presents a significant technical challenge. Some of the fundamental issues include material compatibility and novel packaging concepts to integrate the technical solution into a viable package. Package integrated PCMs can lead to significant system performance increases for any transient system but determining where and how they should be integrated is challenging. In this study, the PCMs will be integrated directly in contact with the top of the heat dissipating die while also maintaining a low thermal packaging resistance to the heat sink. The geometry used in the

analysis is shown in Fig. 3 with a 1 cm x 1 cm silicon chip (k = 120 W/mK) on top of a 3 cm x 3 cm copper heat spreader. The heat is located as a heat flux (100 W/cm^2) on the top of the chip and a heat transfer coefficient (1000 W/m^{2}K) is located on the bottom of the heat spreader. A heat transfer coefficient of 10 W/m^{2}K was assumed on all other surfaces. The ambient and fluid temperatures are both assumed to start at 20°C. The material properties used in the analysis are shown in Table 1.

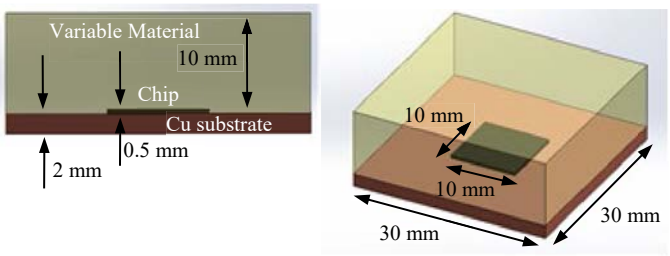

Fig. 3. Geometry and dimensions used in this analysis

Table 1. Material properties used in the analysis

	Copper	Gallium	PT29
Thermal Cond.(s) (W/mK)	390	33.7	0.25
Thermal Cond.(l) (W/mK)	N/A	24	0.15
Density(s) (kg/m^3)	8900	5903	940
Density(l) (kg/m^3)	N/A	6093	850
Specific Heat(s) (J/kgK)	390	340	1770
Specific Heat(l) (J/kgK)	N/A	397	1940
Latent Heat (J/kg)	N/A	80300	202000
Melting Point (°C)	N/A	29.8	29
Reference		[20]	[21]

The focus of this work is on understanding how and where metallic and organic PCMs should be placed into the electronics package. To this end, a series of encapsulant geometries has been investigated with m-PCM (gallium), o-PCM (PT29), and copper placed in various locations in the encapsulation, as is shown in Fig. 4. Gallium and PT29 were chosen because they have the same melting temperature and their properties are well defined which allows for an easy comparison. While the analysis is performed on these two materials, similar conclusions can be made for any m-PCM and o-PCM system with similar melting points. Due to the symmetric nature of the geometry, all cases chosen have both x and y symmetry. In the z-direction, only one material type is chosen to simplify the analysis. Cases 1-3 are a single material: PT29, Cu, and gallium respectively. Cases 4-6 vary the material on top of the chip compared to the material on the encapsulation. Cases 7-9 add copper enhancement into the gallium directly in contact with the chip and allow the o-PCM around the perimeter. Cases 10-12 allow the gallium on top of the chip and around the perimeter with a PT29 layer in between on top of the substrate. Cases 13-15 only have PCM and vary the geometry to increase heat transfer into the o-PCM materials from the m-PCMs.

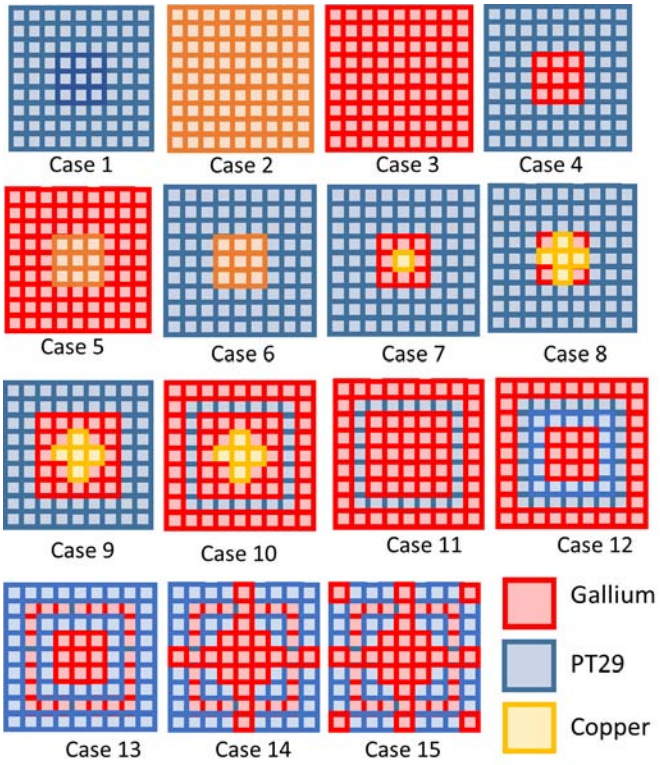

Fig. 4: Encapsulant geometries used in the comparison.

The cases presented in Fig. 4 are not intended to be physically realizable but are intended to demonstrate the concept of time-scale matched PCMs. Future work will investigate integration challenges which could include design rules and/or dielectric materials to ensure the devices maintain electrical performance and additive manufacturing techniques.

MODELING RESULTS

Each of the material configurations in Fig. 4 will be analyzed from 0-300 seconds and compared to their maximum chip temperature and weight to understand the tradeoffs.

Single Material Analysis

Cases 1-3 will be analyzed first (Case 1 = organic PCM, Case 2 = Copper, Case 3 = Gallium) and compared to a gel encapsulant which would typically be used to encapsulate a chip in a power module. Fig. 5 shows the maximum chip temperature at each time step up to 300 seconds. The maximum is calculated as the maximum temperature at any location on the chip and will most likely be located at the top center of the chip. As can be seen in the figure, the encapsulant always results in the highest temperature and the PT29 has a slightly lower temperature. The tradeoff between copper and gallium is more complicated such between ~13-110 seconds, the gallium outperforms the copper but the copper creates a lower temperature outside of those pulse times. This is due to the latent heat absorption of the gallium during the melt which can have a large impact on the temperature. The different steady state values are due to the different package thermal resistances and the thermal conductivity values of the various materials. By the time each solution has reached steady state, the gallium has completely melted but the majority of the PT29 has not yet

melted. This indicates the need for better thermal packaging if it is desired to allow the benefits of both the o-PCM and m-PCM.

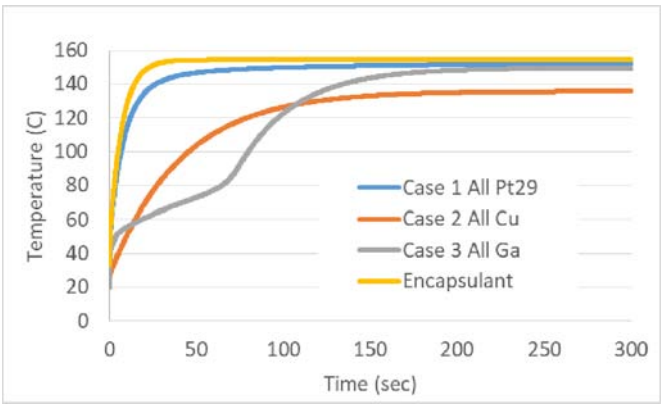

Fig. 5. Maximum chip temperature versus time plot comparing a standard gel encapsulant to all PT29 (organic PCM), all copper, and all gallium (m-PCM).

The temperature is not the only consideration when choosing the material, the weight should also be considered. The weights of each of the encapsulating materials are as follows:

- Case 1 (o-PCM) weight: 8.41g
- Case 2 (Cu) weight: 78.7g
- Case 3 (m-PCM) weight: 52.8g

As this shows, the gallium can both lower the weight as well as the temperature if designed properly.

Multiple Material Analysis

Each of these three materials have their advantages and disadvantages so this section will investigate how to leverage each of their advantages. Organic PCMs (PT29) have very low density and therefore are lightweight, copper has very good thermal conduction and therefore can effectively transfer heat, and gallium has very good latent heat and therefore can absorb heat during a melt. Cases 4-15, shown in Fig. 4, investigate various configurations of integrating each of these materials together and compare them to the Cases 1-3 previously discussed. The results of each of the cases is plotted in Fig. 6. As can be seen, there are now many solutions that outperform copper as well as one (Case 5) which outperforms gallium at some points in time due to the addition of copper over the chip surface.

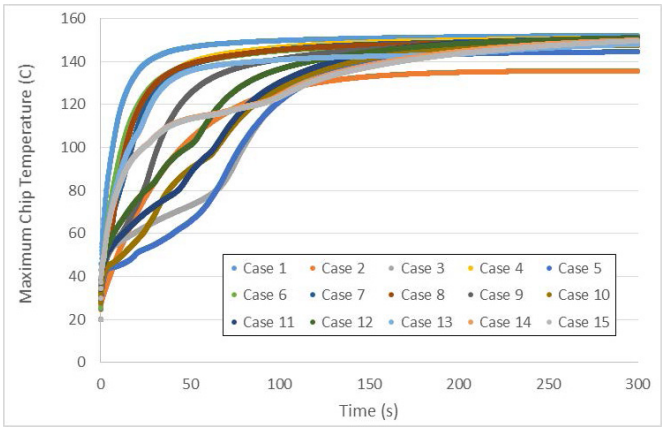

Fig. 6: Maximum temperature versus time for each of the 15 cases.

In order to understand the impact on the weight of each of these cases, the following figures plot the maximum chip temperature versus weight at 1 second (Fig. 7), 10 seconds (Fig. 8), 50 seconds (Fig. 9) and 300 seconds (Fig. 10). The point on the far left is pure paraffin and the point on the far right is pure copper which demonstrate both extremes. Fig. 8 and Fig. 9 show significant temperature deviation between the heaviest and lightest solutions such that it is critical to determine the best solution based on the application. By the time all solutions reach steady state, there is only about 10°C difference between all the solutions and the weight should be the primary consideration at this point. In most pulsed applications, it is clear that a combination of materials is probably the optimal solution.

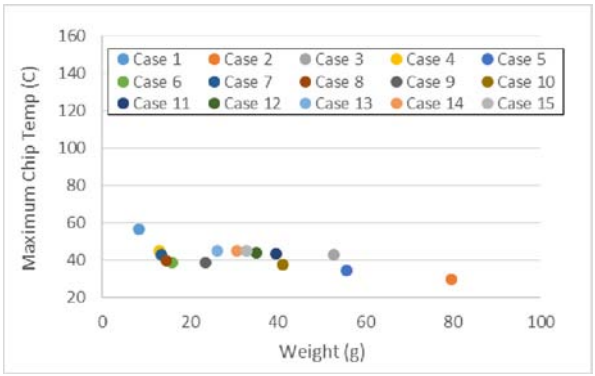

Fig. 7: Maximum chip temperature at 1 second vs. weight

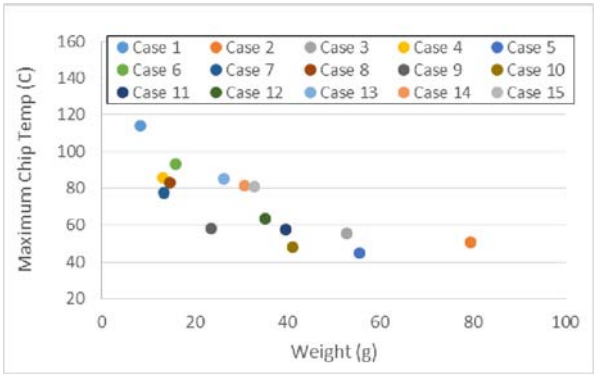

Fig. 8: Maximum chip temperature at 10 seconds vs. weight

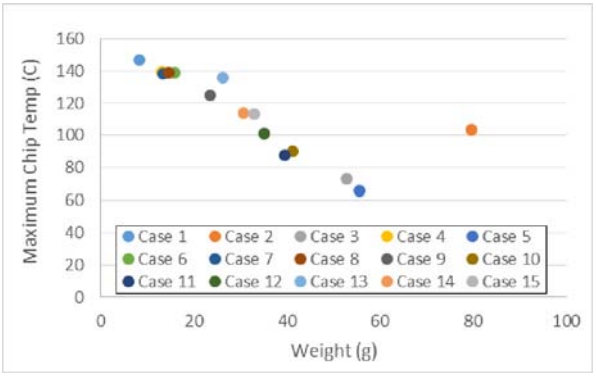

Fig. 9: Maximum chip temperature at 50 seconds vs. weight

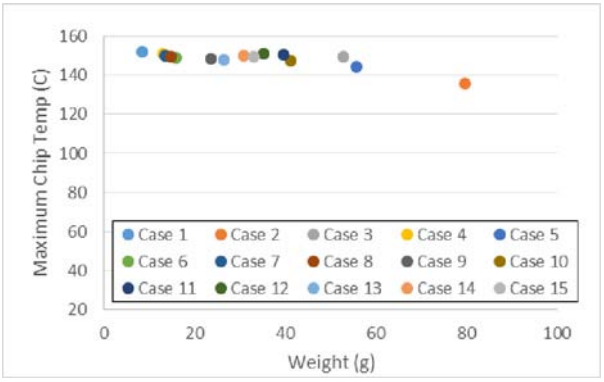

Fig. 10: Maximum chip temperature at 300 seconds (steady state) vs. weight

The reason that combining materials is the optimal solution is due to the time-scale matching of the metallic and organic phase change materials. Time-scale matched PCMs incorporate metallic PCMs in conjunction with organic PCMs to leverage the benefits of each material. Time-scale matching allows the high-k metallic PCMs to quickly absorb the initial portion of the pulse (primary melt) while accommodating the slower heating of the low-k organic PCMs until they also melt (secondary melt) thus allowing a weight saving solution.

TIME SCALE MATCHING REGIMES

The heat transfer process is broken down into 5 distinct regimes after the thermal pulse is initiated: (1) sensible heating of both the m-PCM and o-PCM (2) melting of the m-PCM, sensible heating of the o-PCM (3) melting of the m-PCM and o-PCM (4) sensible heating of the liquid m-PCM and melting of the o-PCM and (5) sensible heating of the liquid m-PCM and o-PCM. These 4 regimes will be demonstrated by looking into more detail at Case 11. Case 11 is shown in Fig. 4 to include gallium (m-PCM) in the center and around the perimeter with a PT29 (o-PCM) layer in between. This configuration is 25% lighter than pure gallium and 50% lighter than pure copper but for many pulses lengths, it performs better than the copper as can be seen in Figure 11; a time versus temperature plot comparing all copper, all gallium and Case 11. The temperature benefit depends on the pulse time as is shown in Figure 11. While Case 11 does not reduce the temperature when compared to all gallium, the significant weight savings could justify its selection.

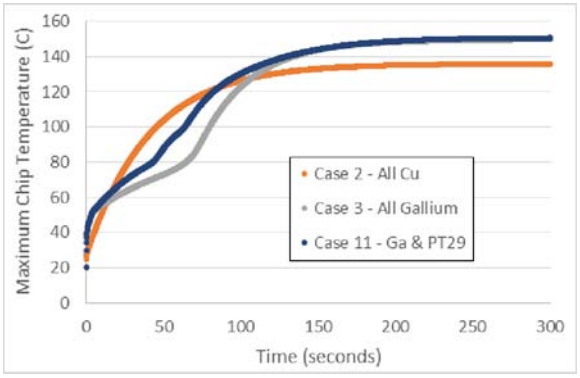

Figure 11: Plot comparing the time versus maximum chip temp for all Cu (orange), all gallium (grey), Case 11 (blue)

For Case 11, the time of first regime (1) – sensible heating of both the m-PCM and o-PCM – is small since the m-PCM is in direct contact with the heat dissipating surface and there is only a small delta between the starting temperature (20°C) and the melting temperature (29°C) allowing the melting to initiate quickly. Figure 12 a and b show the temperature profile and melt fraction profile, respectively, at 0.3 seconds. The figure is oriented such that the m-PCM and o-PCM that are in contact with the chip and the substrate are visible. As can be seen in Figure 12b, there is a very small amount of melting that has already initiated on the surface of the chip, the element directly on the chip surface is about 3% melted, but the majority of both PCMs have not started melting. Figure 12a shows the sensible heating on the m-PCM as well as slight heating on the o-PCM.

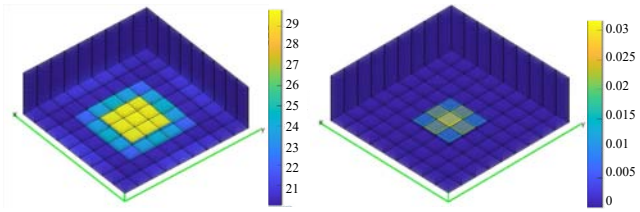

Figure 12. (a) Temperature profile and (b) melt fraction after 0.3 seconds of the m-PCM and the o-PCM.

The second regime (2) – melting of the m-PCM, sensible heating of the o-PCM – occurs for a longer duration than the first regime in this case. Figure 13 a and b show the temperature and melt fraction profile, respectively, at 7 seconds. As can be seen in Figure 13b significant melting of the m-PCM has occurred, mostly in the center above the chip where many elements have a melt fraction of 1 which means they are fully melted. Many m-PCM elements around the perimeter are also 40-50% melted but the o-PCM has not yet started melting. As is seen in Figure 13b, the o-PCM is sensibly heating. This regime continues until 11 seconds at which point the o-PCM begins to melt.

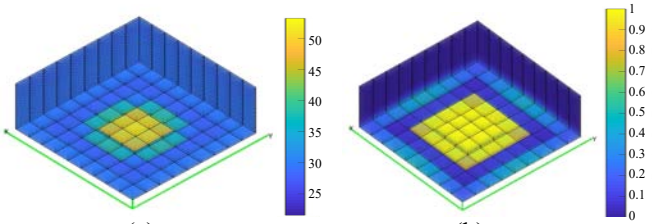

(a) (b)

Figure 13. (a) Temperature profile and (b) melt fraction after 7 seconds of the m-PCM and o-PCM

The third regime (3) – melting of both the m-PCM and o-PCM occurs for the longest duration in this case. It starts at 11 seconds and ends at 60 seconds at which point the metallic PCM has fully melted. Figure 14 and Figure 15 shows the temperature profile and melt fraction, respectively, of both the top and the bottom of the PCM configuration. Both the m-PCM and o-PCMs are melting. The center gallium has fully melted but the exterior ring is still melting as is the PT29. The gallium is helping transfer heat into the PT29.

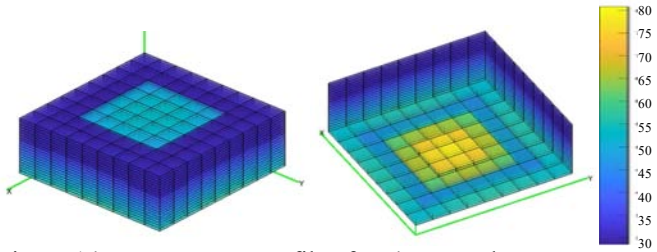

Figure 14. Temperature profile after 45 seconds.

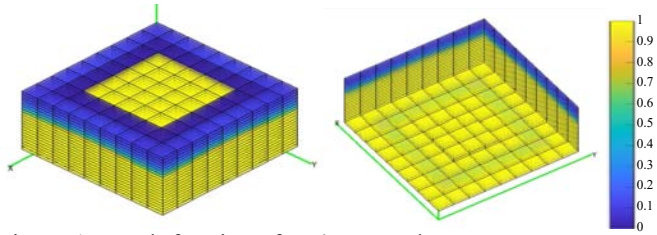

Figure 15. Melt fraction after 45 seconds.

The fourth regime (4) – sensible heating of the liquid m-PCM and melting of the o-PCM, starts around 60 seconds in this case when the gallium is fully melted and ends around 100 seconds when both the m-PCM and o-PCM have fully melted.

The fifth regime (5) – sensible heating of both the liquid m-PCM and o-PCM occurs once all PCM has fully melted and starts around 100 seconds for Case 11. Figure 16 shows the temperature profile at 100 seconds.

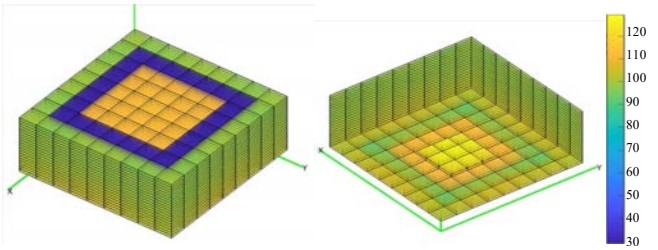

Figure 16. Temperature profile after 100 seconds once all the PCM has melted.

Designing solutions to effectively transfer heat into the o-PCM through the m-PCM can effectively lower the weight while allowing performance tradeoffs with the maximum temeprature. It is necessary to determine the correct confiuration of materials for the pulse application of interest. This will next be investigated with a Monte Carlo simulation where all materials are allowed to vary and an optimal configuration is determined for a 1 second pulse.

MONTE CARLO MATERIAL PLACEMENT STUDY

For a given application, a package should be able to be designed which incorporates gallium, copper and paraffin such that the temperature and weight objectives can be achieved. In order to accomplish this, a limited scope Monte Carlo-based study was executed, serving to support two objectives. First: to provide an additional avenue towards better defining the approaches, design guidelines, and possible benefits of time scale matching metallic and organic PCMs within a package or system. Second: to understand and demonstrate the capabilities allowed ARL ParaPower.

One challenge to taking advantage of timescale matching is the case-by-case nature of any particular application. Design constraints and performance criteria will necessarily dictate what – if any – synergy is to be had from using more than one phase change material. Complicating this is the need to start with some preconceived arrangement of the different materials to start probing for possible benefits. One alternative is to instead let a series of simulations suggest possible arrangements, rather than rely on such preconceptions.

A two-dimensional variation of the geometry modeled above was assumed with a 500 µm thick Si chip on a 1 mm thick Cu spreader with backside heat transfer coefficient of 1000 W/m^2-K. The half width of the chip is 0.5 cm, and the spreader twice that at 1 cm. Overlaying the chip and spreader is an encapsulation region bringing the total system thickness to 3.5 mm. All boundaries but the bottom are insulated (the left boundary representing mirror symmetry), and the chip dissipates 200 W/cm^2 at its upper surface (adjacent to the encapsulant). The target model timescale to optimize for was 1 second. Initial temperature and the convection ambient are 15°C. The two-dimensional assumption did lead to higher temperatures in the system as lateral heat spreading was restricted from what was two directions to

The materials used within the encapsulant region are organic paraffin PT29, metallic gallium, and/or copper (acting as conductivity enhancement). Since both the volumetric (sensible) heat capacity and volumetric latent heat of gallium is larger than that of the paraffin, it is a thermally superior phase change material. Possible advantages of using paraffin must then stem from its lighter weight and lower cost. To this end the two competing performance criteria chosen were maximum system temperature and system weight. When plotting possible designs on a two dimensional performance space, a Pareto front emerges representing the tradeoff between weight and thermal performance. Any model configuration lying on this front will be strictly superior to cases that lie above and to the right.

The stochastic element to the simulation is the material placement within the encapsulant region. In each of the 510

finite elements representing this region the material assigned one of the three materials. Initial attempts using independent uniform selection for each element lead to a large central tendency of unstructured models that underperform compared to simple handcrafted test cases (e.g. a layer of gallium followed by a layer of paraffin). Thus an iterative approach was adopted where the current Pareto front is evolved by repeatedly reassigning a random subset (of a tunable size ranging from 5% – 0.5%) of the elements of each out-performing case and establishing a new front from the results. Since this approach makes it difficult to explore the farthest reaches of the design space (e.g. all gallium or all paraffin) a combined approach is used where five handcrafted seed cases are used to initialize the evolution process.

The evolution of the Pareto front becomes negligable after an overnight HPC run (~8 hours). Typical simulation parameters consist of 100,000 trial cases to be simulated based off those on the current Pareto front, and for the trial/update process to be iterated 1000+ times. That tens of millions of simulations are possible in such a short time frame is due to the fast matrix assembly and inversion used by the ParaPower PCM solver.

Figure 17 is an example of a converged Pareto front (red) for a 1 second pulse, accompanied by 30,000 trial cases (scattered points to the right and above the front). The encapsulant composition of each trial cases by percent volume is designated by RGB values with red = copper, green = gallium, and blue = paraffin. Also shown are thermal results for the same cases taken at different time snapshots, illustrating that configurations that are "optimal" at 1 second are not necessarily so at other timescales. For example, the cluster marked with the green arrow at 0.25 seconds stems from the 100% gallium seed case. The seed case lies in advance of the front cases at 0.25 seconds, but then underperforms similar weight configurations containing (structured) small percentages of paraffin and Cu at 1 second.

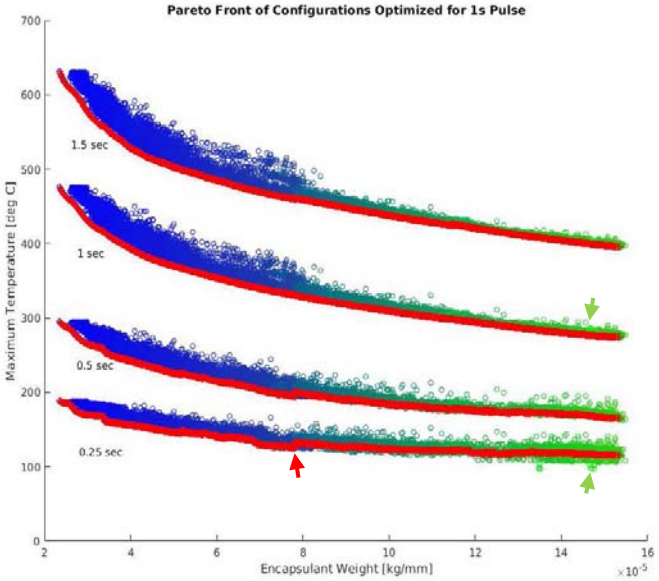

Figure 17: Pareto front optimized at 1 second then also shown at 0.25, 0.5 and 1.5 seconds.

Also of interest is the emergence of "families" of configurations, as evidenced by the jump discontinuities in the front case responses at low timescales (e.g. at the red arrow). It is likely the families stem from the different initial seed cases, and the strict selection criteria (always keep optimal) and low degree of re-randomization of each trial leads to a hill-climbing algorithm where each family fills a niche and it is difficult (improbable) to jump into alternative basins of optimality.

Looking a little more into the "families", Figure 18, shows the optimized configurations fom the two families straddling the red arrow of Figure 17. Case 646 is related to the paraffin rich family just to the left of the red arrow, while case 647 is from the more gallium rich family to the right of the arrow. The cases chosen are at the common niche boundary of these two families, and so have effectively the same encapsulant weight at 1 second. Case 646 strictly outperforms case 647 a timescales shorter than 1 second, although there are likely new optimal cases to be found if one explcitly optimizes for e.g. 0.25 s duration.

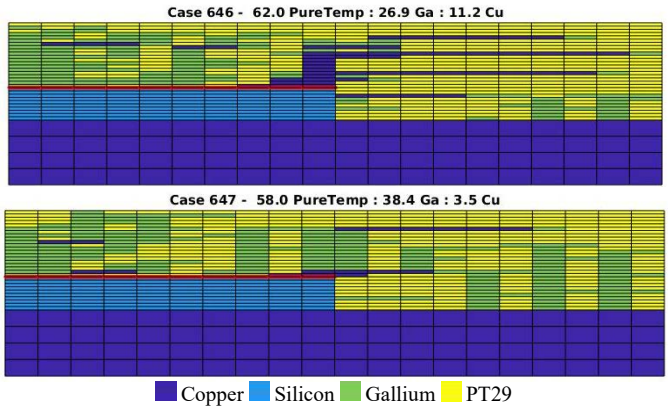

Figure 18: Two families of solutions that have the same weight and performance but one shows copper fins into the organic PCM and the other shows gallium fins into the organic PCM.

Also demonstrated is the high degree of structure found in the Pareto front cases. Copper inclusions are used judiciously to create finned enhancement structures concentrated at the corner of the chip. The gallium and paraffin tend to be arranged in alternating columns, radiating in directions aligned with the predominant pathways of heat into the encapsulant region. These structures are selected for automatically by the iterative Monte Carlo algorithm.

SUMMARY AND CONCLUSIONS

By integrating PCMs with the electronics package, the overall system can be improved by reducing the heat sink and cooling requirements and/or increasing dissipated power density while at the same time ensuring the device temperature does not exceed its limit under pulsed loading conditions. This work is novel in that it proposes a time-scale matched approach which incorporates m-PCMs in conjunction with o-PCMs to leverage the benefits of each. Combining organic and metallic PCMs into a single thermal system has not been shown before. Time-scale matching allows the high-k m-PCMs to quickly absorb the initial portion of the pulse while accommodating the

slower heating of the low-k o-PCMs to optimize weight and performance. In addition, an iterative Monte Carlo method was used to find optimal packages that use a paraffin/gallium/copper composite system in place of traditional encapsulation. The enabling technology for this study is the fast solving ParaPower model, allowing quick parametric analysis including tens of millions of cases to be executed and analyzed within the course of an eight-hour HPC job submission.

Acknowledgments

The authors would like to acknowledge Bruce Geil (Army Research Laboratory), the Office of Naval Research and the Office of the Secretary of Defense for supporting the research.

References

[1] L.M. Boteler and D. Sharar, "Thermal and Packaging Challenges of Power Electronics Modules" In Gomac Tech 2016 Proceedings, pp. 14-17, 2016

[2] Chukwu, S., Ogbonnaya, E., & Weiss, L. (2012, July). Fabrication, Testing, and Enhancement of a Thermal Energy Storage Device Utilizing Phase Change Materials. In ASME 2012 Heat Transfer Summer Conference collocated with the ASME 2012 Fluids Engineering Division Summer Meeting and the ASME 2012 10th International Conference on Nanochannels, Microchannels, and Minichannels (pp. 279-285). , doi:10.1115/HT2012-58309.

[3] Shuja, S. Z., Yilbas, B. S., & Shaukat, M. M. (2015). Melting enhancement of a phase change material with presence of a metallic mesh. Applied Thermal Engineering, 79, 163-173.

[4] Zhao, C. Y., Lu, W., & Tian, Y. (2010). Heat transfer enhancement for thermal energy storage using metal foams embedded within phase change materials (PCMs). Solar Energy , 84 (8), 1402-1412.

[5] Setoh, G., Tan, F. L., & Fok, S. C. (2010). Experimental studies on the use of a phase change material for cooling mobile phones. International Communications in Heat and Mass Transfer , 37 (9), 1403-1410.

[6] Fleischer, A. S., Chintakrinda, K., Weinstein, R., & Bessel, C. A. (2008, May). Transient thermal management using phase change materials with embedded graphite nanofibers for systems with high power requirements. In Thermal and Thermomechanical Phenomena in Electronic Systems, 2008. ITHERM 2008. 11th Intersociety Conference on (pp. 561-566).

[7] Xie, B., Cheng, W. L., & Xu, Z. M. (2015). Studies on the effect of shape-stabilized PCM filled aluminum honeycomb composite material on thermal control. International Journal of Heat and Mass Transfer , 91 , 135-143.

[8] Jankowski, N. R., & McCluskey, F. P. (2014). A review of phase change materials for vehicle component thermal buffering. Applied Energy, 113, 1525-1561.

[9] Ge, H.; Li, H.; Mei, S. & Liu, J. Low melting point liquid metal as a new class of phase change material: An emerging frontier in energy area Renewable and Sustainable Energy Reviews, 2013, 21, 331-346.

[10] Lu, T. J. Thermal management of high power electronics with phase change cooling, International Journal of Heat and Mass Transfer, 2000, 43, 2245-2256,

[11] Shamberger, P. J. (2016). Cooling Capacity Figure of Merit for Phase Change Materials. Journal of Heat Transfer , 138 (2), 024502.

[12] Shao, L., Raghavan, A., Kim, G. H., Emurian, L., Rosen, J., Papaefthymiou, M. C. & Pipe, K. P. (2016). Figure-of-merit for phase-change materials used in thermal management. International Journal of Heat and Mass Transfer, 101, 764-771.

[13] Krishnan S, Garimella SV. Thermal Management of Transient Power Spikes in Electronics—Phase Change Energy Storage or Copper Heat Sinks?. ASME. *J. Electron. Packag.* 2004;126(3):308-316.

[14] Evans, A. G., He, M. Y., Hutchinson, J. W., & Shaw, M. (2001). Temperature distribution in advanced power electronics systems and the effect of phase change materials on temperature suppression during power pulses. Journal of Electronic Packaging, 123(3), 211-217.

[15] Gonzalez Nino, D., Boteler, L., Ibitayo, D., Jankowski, N. R., & Quintero, P. O. (2016, July 10-14). "Numerical Evaluation of Multiple Phase Change Materials for Pulsed Electronics Applications." ASME 2016 Summer Heat Transfer Conference.

[16] David Gonzalez-Nino, Lauren M. Boteler, Dimeji Ibitayo, Nicholas R. Jankowski, Damian Urciuoli, Iain M. Kierzewski, Pedro O. Quintero, "Experimental evaluation of metallic phase change materials for thermal transient mitigation," International Journal of Heat and Mass Transfer,Volume 116, 2018, Pages 512-519, ISSN 0017-9310,

[17] L. M. Boteler and S. M. Miner, "Power packaging thermal and stress model for quick parametric analyses," in Proceedings of the ASME 2017 International Technical Conference and Exhibition on Packaging and Integration of Electronic and Photonic Microsystems InterPACK, pp. 1-8, 2017

[18] L. Boteler, A. Smith, "3D thermal resistance network method for the design of highly integrated packages", Proc. ASME Summer Heat Transf. Conf., pp. 1-9, 2013

[19] Deckard, M. Fish, M., Berman, M. Wang, J., Boteler, L., Shamberger, P. "Convergence and Validation in ParaPower: A Design Tool for Phase Change Materials in Electronics Packaging", ITherm Proceedings 2019.

[20] "PubChem Compound Database," 18 December 2018. [Online]. Available: https://pubchem.ncbi.nlm.nih.gov/compound/5360835.

[21] "PureTemp 29 technical data sheet," 2018. [Online]. Available: http://www.puretemp.com/stories/puretemp-29-tds.